01 Jan 2023

Mode-Decomposition-Based Equivalent Via (MEV) Model and MEV Model Application Range Analysis

Chaofeng Li

Kevin Cai

Muqi Ouyang

Manish Kizhakkeveettil Mathew

et. al. For a complete list of authors, see https://scholarsmine.mst.edu/ele_comeng_facwork/5140

Recommended Citation

C. Li et al., "Mode-Decomposition-Based Equivalent Via (MEV) Model and MEV Model Application Range Analysis," *2023 Joint Asia-Pacific International Symposium on Electromagnetic Compatibility and International Conference on ElectroMagnetic Interference and Compatibility, APEMC/INCEMIC 2023*, Institute of Electrical and Electronics Engineers, Jan 2023.
The definitive version is available at https://doi.org/10.1109/APEMC57782.2023.10217672

Mode-decomposition-based Equivalent Via (MEV) Model and MEV Model Application Range Analysis

Chaofeng Li[#1], Kevin Cai[*2], Muqi Ouyang[#3], Manish Kizhakkeveettil Mathew[#4], Mehdi Mousav[#5], Bidyut Sen[*6], DongHyun Kim[#7]
[#]EMC Laboratory, Missouri University of Science and Technology, Rolla, MO, USA
[*]Unified Computing System, Cisco System, Inc, San Jose, CA, USA
[1]clf83, [3]muqio, [4]mkmbzm, [5]smousavi, [7]dkim@mst.edu
[2]kecai, [6]bisen@cisco.com

2023 Joint Asia-Pacific International Symposium on Electromagnetic Compatibility and International Conference on ElectroMagnetic Interference & Compatibility (APEMC/INCEMIC) | 979-8-3503-3834-8/23/$31.00 ©2023 IEEE | DOI: 10.1109/APEMC57782.2023.10217672

***Abstract*—The mode-decomposition-based equivalent via (MEV) model is proposed in this paper, which is a physics-based equivalent model for the high-speed channel modeling. The application ranges of the MEV model are analyzed by varying anti-pad radius, via radius, and distance between the parallel plates for a single via with multiple layers. Based on the S-parameter comparison with full-wave simulations, the MEV model is useful for the insertion loss calculation up to 100 GHz. Meanwhile, the return loss from the MEV model shows a high level of correlation with full-wave simulation results up to 70GHz, even when the anti-pad radius is larger than the commonly used size. The parallel-plate height has a negligible impact on the accuracy of the MEV model. This paper demonstrates the large application range of the MEV model and verifies that MEV model is suitable for practical high-speed via analysis.**

Keywords—mode-decomposition, parallel plate mode, high-order modes, equivalent via model, high-speed channel

I. Introduction

Transition via is commonly used in high-speed printed circuit boards (PCB), which can significantly impact the signal integrity of high-speed circuits [1]. It is very important to model and analyze the via performance at the pre-design stage for signal integrity of the high-speed channels. To overcome the long computation time, physics-based equivalent via model has been developed for many years, which can not only save time compared with full-wave numerical simulation methods, but also provide physics-based insight as via design guideline. However, the conventional physics-based via model is no longer accurate in high frequency, such as frequency over 20 GHz, because the parallel-plate impedance is calculated based on only the fundamental parallel-plate mode [2]. To improve the accuracy of the conventional physics-based equivalent model, Williamson [3] and Zhang [4] proposed more complex equivalent circuits for via structures by considering higher-order modes in the vicinity of the via domain. However, extracting the circuit elements for the two models is complex, and the circuit models are still not accurate beyond 40 GHz for typical PCB via dimensions [2].

A mode-decomposition-based equivalent via (MEV) model is proposed for high-speed channel modeling, which is also a physics-based equivalent model [7]. The MEV model is different from the conventional physics-based via model. The high-order parallel-plate modes are modeled as the parallel-plate impedance Z' in the MEV model based on the newly proposed mode-decomposition method, as shown in Figure 1. Thus, the MEV model meets the high-accuracy and the high-bandwidth requirements compared with the conventional equivalent via models. The MEV model is introduced in section II. In section III, S-parameters are compared to deduce application range of the MEV model. In addition, the relative error in the S-parameter from the MEV model and HFSS are analyzed. Finally, the conclusion of the paper is given in section IV.

II. The Proposed MEV Model

Based on the conventional physics-based method, a segment cell of the via can be modeled using a π-type equivalent circuit including two capacitors and the parallel-plate impedance based on domain decomposition method. Fig. 1 shows the proposed MEV model for the fundamental cell of a via, which corresponds to via segment crossing a cavity enclosed by two reference plates. The equivalent model includes four capacitors and the parallel-plate impedances Z_{p0} and Z'. Z_{p0} and Z' are parallel-plate impedance due to the fundamental parallel-plate mode and higher-order parallel-plate modes in the parallel-plate domain, respectively. C_a represents the coupling capacitance for the anti-pad domain meanwhile C_b is the coupling capacitance between the via barrel and the top or bottom reference plate. Unlike the conventional physics-based model, the proposed MEV model considers the impact of higher-order modes, which means the MEV model can work with high accuracy and high bandwidth.

The coupling capacitance between the via barrel and the parallel plate has been analyzed for many years. Many methods have been developed for calculating the via-plate capacitance of a via structure [5]-[6]. In this paper, the anti-pad capacitance C_a and the via barrel-plate capacitance C_b are calculated as shown below [6].

$$C_a = \frac{2\pi\varepsilon_0\varepsilon_r t}{ln(\frac{r_a}{r_p})} \tag{1}$$

$$C_b = \frac{j4\pi^2\varepsilon_0\varepsilon_r}{\left(ln\left(\frac{r_a}{r_p}\right)\right)^2 h}\sum_{n=1,3,5}^{\infty}\frac{\tilde{K}_n}{\tilde{k}_n} \tag{2}$$

where

979-8-3503-3834-8/23/$31.00 ©2023 IEEE

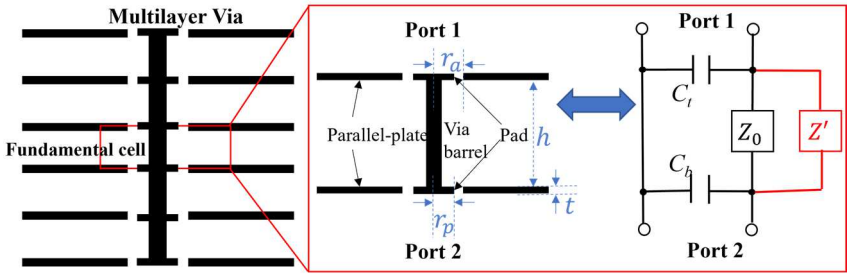

Fig. 1. Mode-decomposition-based equivalent model for the fundamental cell of the via.

$$\tilde{k}_n = -\frac{jn\pi}{h} \tag{3}$$

$$\tilde{K}_n = \frac{1}{\tilde{k}_n}\begin{pmatrix} \frac{2jln(r_a/r_p)}{\pi} - H_0^2(\tilde{k}_n r_a)J_0(\tilde{k}_n r_a) \\ -H_0^2(\tilde{k}_n r_p)J_0(\tilde{k}_n r_p) + 2H_0^2(\tilde{k}_n r_a)J_0(\tilde{k}_n r_p) \\ +\frac{J_0(\tilde{k}_n r_0)}{H_0^2(\tilde{k}_n r_0)}\left(H_0^2(\tilde{k}_n r_a) - H_0^2(\tilde{k}_n r_p)\right)^2 \end{pmatrix} \tag{4}$$

where r_a, r_0 and r_p are the anti-pad, via and pad radii, respectively. h is the parallel-plate height, which corresponds to the distance between the two parallel plates. t is the plate thickness. ε_0 and ε_r are the free space permittivity and relative permittivity of the dielectric, respectively. H_0^2 and J_0 are the zero-order Hankel function of the second kind and the zero-order Bessel function.

The parallel-plate impedance Z_{p0} represents the coupling between the via and the parallel-plate due to the fundamental parallel-plate mode, which can be calculated by the modal fields. When the parallel plate is infinitely large or the boundary condition of the plate consists of perfectly matched layers (PMLs), we can calculate the parallel-plate impedance Z_{p0} as

$$Z_{p0} = \frac{V_0}{I_0} = \frac{-E_z^0 h}{2\pi r_0 H_\emptyset^0} \tag{5}$$

where V_0 and I_0 are the voltage and current at the via-barrel boundary due to the fundamental mode. E_z^0 and $H_\emptyset^0$ represent the electric and magnetic fields at the via-barrel boundary due to the fundamental mode.

$$E_z^0(r_0) = k_0^2 a_0 H_0^2(k_0 r_0) \tag{6}$$

$$H_\emptyset^0(\mathrm{r_0}) = j\omega\varepsilon_0\varepsilon_r k_0 a_0 H_1^2(k_0 r_0) \tag{7}$$

Here, $k_0 = k' - jk''$ is a complex wavenumber, $k' = \omega\sqrt{\mu_0\varepsilon_0\varepsilon_r}$ and $k'' = \omega\sqrt{\mu_0\varepsilon_0\varepsilon_r}(tan\delta + \frac{d_s}{h})/2$, ω is the angular frequency, μ_0 is the permeability of free space, $tan\delta$ is the loss tangent of the material, $d_s = \sqrt{2/\omega\mu_0\sigma}$ is the skin depth of conductor with conductivity of σ, a_0 is a constant coefficient that does not need to be determined, and H_1^2 is the first-order Hankel function of the second kind. When the parallel plate is finite or the boundary condition of the plate is a perfect electric or magnetic conductor (PEC or PMC) boundary, the parallel-plate impedance can be calculated based on the cavity method.

Unlike the fundamental mode, the higher-order parallel-plate modes are excited at the anti-pad boundary. For the higher-order modes, only TM_{0n} modes are considered. Because the via structure under consideration is a cylinder, which is symmetric, only TM_{0n} modes (higher-order modes/axially isotropic modes) are excited [4]. Similar to the parallel-plate impedance calculation of the fundamental mode, the higher-order mode impedance can also be calculated by using the voltage and current at the anti-pad boundary.

$$Z' = \frac{V_a}{I_a} = \frac{h\sum_{n=1}^{N} k_n H_0^2(k_n r_a)}{j2\pi r_a \omega\varepsilon_0\varepsilon_r \sum_{n=1}^{N} H_1^2(k_n r_a)} \tag{8}$$

where V_0 and I_0 are the voltage and current at the via-barrel boundary due to the fundamental mode. r_a is the anti-pad radius, $k_n = \sqrt{k_0^2 - (n\pi/h)^2}$, n represents the mode number, N is the total number of higher-order modes considered for the via modeling. The derivation details of Z' can be found in the reference [11].

III. Applications and Analysis

A sample case, single via with 4 layers, is used to investigate the proposed MEV model, as shown in Figure 2. To simplify the analysis, the via model does not have any via pad. The relative permittivity ε_r and the loss tangent of the dielectric material are 3.68 and 0.02 at 1 GHz using the Djordjevic model. The conductivity of copper plate is 5.8×10^7. To investigate the application range of the proposed MEV model, the anti-pad radius, the via radius and the parallel-plate heigh are swept, respectively. The insertion loss and return loss is compared between the proposed model and HFSS.

A. Analysis on Varying Anti-pad Radius

For the first part of application analysis, the anti-pad radius r_a is swept from 10 mils to 20 mils with a step of 5 mils. The via radius is fixed as 5 mils, the height of the parallel-plate is fixed as 10 mils and the thickness of the plate is fixed as 1.3 mils. The comparison of the insertion loss and the return loss of the different via models with various anti-pad radii are plotted in

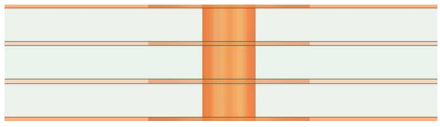

Fig. 2. Cross-section view of single via with 4 layers

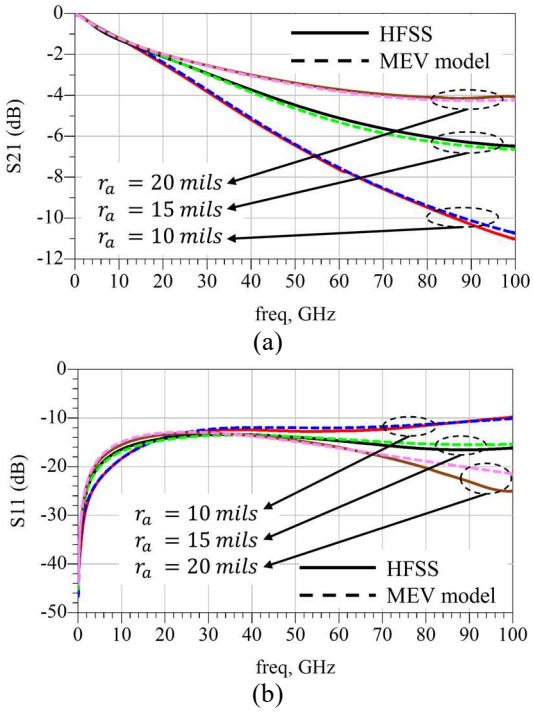

Fig. 3. S-parameters comparison from the proposed MEV model and HFSS: (a) The insertion loss comparison, (b) The return loss comparison.

Figure 3, to compare the proposed analytical MEV model and HFSS simulation results.

The solid curves are the results from HFSS meanwhile the dotted lines represents the results from the MEV model. High level of correlation in insertion loss can be observed for all different via models. However, when the anti-pad radius increase, the observable difference of the return loss can be observed at high frequency range between the results from the MEV model and HFSS because via self-inductance is assumed to be negligible in the equivalent model for high frequencies. When anti-pad radius becomes larger, at high frequency, via self-inductance is no longer negligible.

To evaluate the difference in S-parameters between the MEV model and HFSS in detail, the relative errors of the insertion loss and the return loss are plotted in Figure 4. The relative error is defined as shown below.

$$\sigma = \left| \frac{|S^{HFSS}| - |S^{MEV}|}{|S^{HFSS}|} \right| \times 100\% \qquad (9)$$

where S^{HFSS} is the insertion loss or the return loss from HFSS, S^{MEV} is the insertion loss or the return loss from the MEV model. From the Figure 4 (a), the relative errors of the insertion loss S21 are all less than 5%. However, the relative errors of the return loss S11 could only be less than 10% for the frequency bandwidth of below 70 GHz. The relative error of S11 increase above 70 GHz with the increase of anti-pad radius. We also observe that the relative error of S11 could be large than 10% at very low frequency points, which can be ignored because the magnitude of S11 at these frequency points is very small, less than -40dB.

B. *Analysis on Varying Via Radius*

For the second part of application analysis, the via radius r_0 is swept from 2 mils to 8 mils with a step of 2 mils. The anti-pad radius is fixed as 15 mils, the parallel-plate height and the thickness of the plate are unchanged, and it remains the same as the case of anti-pad sweeping. The relative errors of the S-parameters for all via radius are plotted in the Figure 5. Similar to the cases of anti-pad radius sweeping, the relative errors of S21 remains less than 10% up to 100 GHz for all via radius cases. However, the relative errors of S11 is higher than 10% above 70 GHz for the cases that the via radius is small than 6 mils, which means that the MEV model can only work up to 70 GHz for small via radius cases. From Figure 4 (b), we can observe that the relative errors of S11 increase above 70 GHz with the decrease of anti-pad radius, similar to the cases of anti-pad radius sweeping.

From the analysis results, it becomes clear that the accuracy of the MEV model on S11 calculation is correlated with the ratio of the anti-pad radius to the via radius. The ratio of the anti-pad radius to the via radius is defined as $r_{av} = r_a/r_0$. Only when r_{av} is smaller than 2.5, the MEV model can work up to 100 GHz for S11 calculation. For all other cases, the MEV model can calculate the S11 accurately up to 70 GHz.

C. *Analysis on Varying Parallel-plate Height*

For the last part of application analysis, the parallel-plate height h is swept from 7 mils to 15 mils, which covers most of

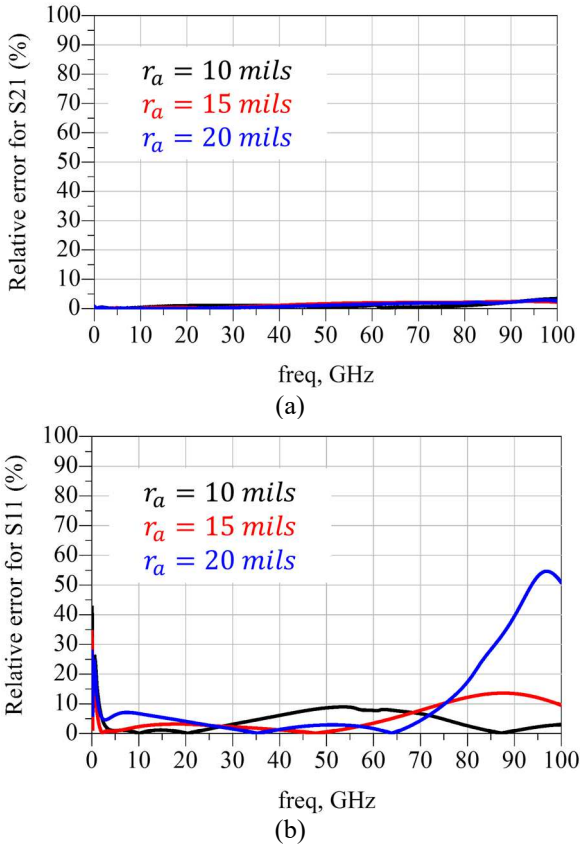

Fig. 4. Relative errors of S-parameters for the cases of varying anti-pad radius: (a) relative errors for S21, (b) relative errors for S11.

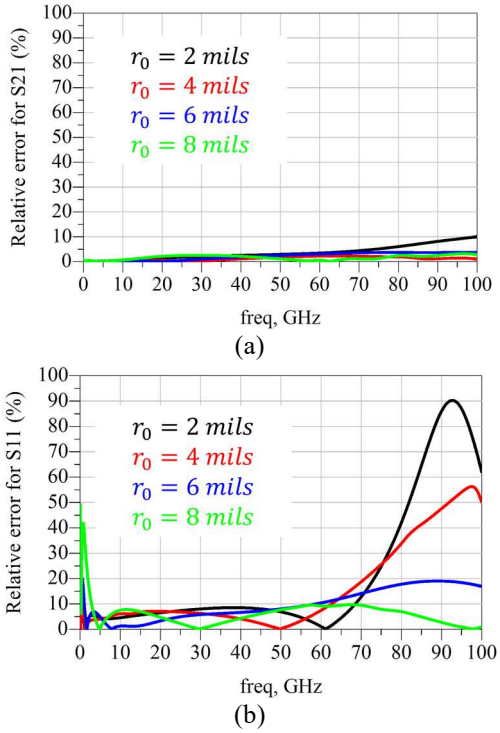

Fig. 5. Relative errors of S-parameters for the cases of varying via radius: (a) relative errors for S21, (b) relative errors for S11.

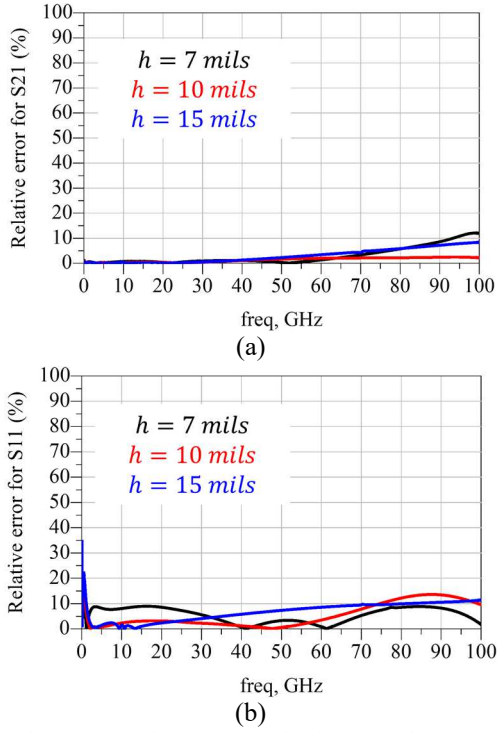

Fig. 6. Relative errors of S-parameters for the cases of varying parallel-plate height: (a) relative errors for S21, (b) relative errors for S11.

practical application ranges for high-speed channels in printed circuit boards and packages. The anti-pad radius is 15 mils, the via radius and the thickness of the plate remains unchanged as the case of anti-pad s weeping. Similar to Figure 5, the relative errors of the S-parameters are plotted in the Figure 6. The relative errors are less than 15% for all cases up to 100 GHz. We can observe that the relative errors of S-parameters are similar for different parallel-plate heights, which means the parallel plate height has a negligible impact on the accuracy of the MEV model.

IV. Conclusion

In this paper, different practical high-speed vias are analyzed using the MEV model, based on the newly proposed domain decomposition and mode decomposition methods. The application ranges of the MEV model are investigated by sweeping the anti-pad radius, the via radius and the parallel-plate height. The MEV model can calculate the S21 of a practical via design up to 100 GHz. The S11 from the MEV model shows high level of accuracy compared to HFSS results up to 70 GHz, even for the via with a large via radius to anti-pad radius ratio. From the analysis, the ratio of the anti-pad radius to the via radius is defined as r_{av} and correlated with the accuracy of the MEV model. When r_{av} is smaller than 2.5, the MEV model can work up to 100 GHz for S11 calculation. In addition, the parallel-plate height has a little impact on the accuracy of the MEV model based on the analysis. Within anti-pad diameter sizes of 20 mils and 40 mils and via diameter sizes of 4 mils and 16 mils, the MEV via model shows less than 10 % error compared to HFSS simulation result, up to 70 GHz. This paper also verifies the possibility of using the MEV model for high-speed via optimization for practical high-speed via sizes.

V. Acknowledgements

This work was supported in part by the National Science Foundation (NSF) under Grant IIP-1916535.

References

[1] S. H. Hall, G. W. Hall, and J. A. McCall, *High-Speed Digital System Design—A Handbook Of Interconnect Theory and Design Practices*. New York, Wiley, 2000, ch. 5, pp. 94–116.

[2] S. Müller, X. Duan, M. Kotzev, Y.-J. Zhang, J. Fan, X. Gu, Y. H. Kwark, R. Rimolo-Donadio, H.-D. Brüns, and C. Schuster, "Accuracy of physics-based via models for simulation of dense via arrays," *IEEE Trans. Electromagn. Compat.*, vol. 54, no. 5, pp. 1125–1136, October 2012, doi: 10.1109/TEMC.2012.2192123.

[3] A. G.Williamson, "Radial-line/coaxial-line junctions: Analysis and equivalent circuits," *Int. J. Electron.*, vol. 58, no. 1, pp. 91–104, 1985, doi: 10.1080/00207218508939005.

[4] Y.-J. Zhang and J. Fan, "An intrinsic circuit model for multiple vias in an irregular plate pair through rigorous electromagnetic analysis," *IEEE Trans. Microw. Theory Tech.*, vol. 58, no. 8, pp. 2251–2265, Aug. 2010, doi: 10.1109/TMTT.2010.2052956.

[5] M. Friedrich, C. Bednarz, and M. Leone, "Improved expression for the via-plate capacitance based on the magnetic-frill model," *IEEE Trans. Electromagn, Compat.*, vol. 55, no. 6, pp. 1362–1364, Dec. 2013, doi: 10.1109/TEMC.2013.2265041.

[6] M. Friedrich,M. Leone, and C. Bednarz, "Exact analytical solution for the via-plate capacitance in multi-layer structures," *IEEE Trans. Electromagn, Compat.*, vol. 54, no. 5, pp. 1097–1104, Oct. 2012, doi: 10.1109/TEMC.2012.2189573.

[7] C. Li, K. Cai, M. Ouyang, Q. Gao, B. Sen and D. Kim. " Mode-Decomposition-Based Equivalent Model of High-Speed Via up to 100 GHz," In Progress of Reviewing by *IEEE Trans. Signal Integrity and Power Integrity*, 2022.